Available online at www.sciencedirect.com
ScienceDirect
Dyes and Pigments 76 (2008) 810–816
DYES and PIGMENTS
www.elsevier.com/locate/dyepig

Synthesis and characterization of perylene tetracarboxylic bisester monoimide derivatives

Xiaobing Zhang, Yangfang Wu, Jianzhong Li, Fan Li, Min Li*

Key Laboratory for Automobile Materials (JLU), Ministry of Education, Department of Materials Science and Engineering, Jilin University, Changchun 130012, PR China

Received 30 November 2006; received in revised form 9 February 2007; accepted 11 February 2007
Available online 2 March 2007

Abstract

The synthesis, optical properties, electrochemical properties and electronic structures of *n*-(1-butyl)perylene-3,4:9,10-tetracarboxylic-3,4-(bis-alkylester)-9,10-imide (C4−C*n*) and 1,3-bis[(*n*-(1-butyl)perylene-3,4:9,10-tetracarboxylic-3-alkylester-9,10-imide)-4-ester] dioxypropane (C4−C3−C4) are reported. Molecular structures of the compounds were confirmed by FT-IR, ^{1}H NMR spectroscopies and elemental analysis. Their optical and electrochemical properties were investigated by UV−vis absorption and fluorescence spectroscopy as well as cyclic voltammetry. C4−C*n* exhibited strong green-yellow fluorescence ($\lambda_{max} = 523$ nm) in dilute solution, while the dimer C4−C3−C4 exhibited orange with maximum emission at 568 nm. Both C4−C*n* and C4−C3−C4 were soluble in common organic solvents such as chloroform and dichloromethane, which is due to the introduction of alkyl chains, compared to perylene. The HOMO and LUMO energy levels of the compounds studied are in the range of −3.76 to −3.79 eV and −5.96 to −6.10 eV. Calculations on the representative compounds by the Dmol^3 package of MS Modeling 3.0 revealed that the increase of energy levels in both C4−C*n* and C4−C3−C4, compared to that of 3,4,9,10-perylene tetracarboxylic dianhydride (PTCDA), is due to the influence of the substituents on the energy band structures of the perylene derivatives, and they are excellent electron-transporting materials.

Keywords: Perylene derivatives; Photoluminescence; Energy level

1. Introduction

Molecular and polymeric organic materials offer substantial advantages over inorganic materials as the emissive components in light-emitting diodes (LEDs), as they are generally more easily processed into device which thus reduces production costs [1]. During the past years, some perylene imides/bisimides have become available with a broad range of optical and electrochemical properties [2,3]. The perylene derivatives are well known organic dyes and pigments used in paints and coatings. Furthermore, their electrical and optical properties, in particular, their strong absorption and emission in the visible region, make them candidates for many applications. For example, perylene imides representing a class of n-type semiconductors exhibiting relatively high electron affinity among large-band-gap materials are potential photoactive and electroactive organic materials. Also, they exhibit high fluorescence quantum yields with excellent photochemical, redox properties [4] and good thermal stability. Currently, the low molecular weight perylene imides are being investigated for use in a variety of technological applications such as optical switching [5], photoreceptors, chemical sensors, electroluminescent devices [6,7], and colorful liquid crystal display [8–11], and have attracted much attention due to their potential applications in organic solar cells [12–17]. While the low solubility of perylene imides in organic solvents limits their utilities in devices, thin films of perylene derivatives could be prepared by vapor deposition method or blending them with polymers. Efforts have been made, such as introducing dendritic structures into the bay positions of perylene core [18–21], to attach solubilizing

* Corresponding author. Tel.: +86 431 85168254.
E-mail address: minli@mail.jlu.edu.cn (M. Li).

0143-7208/$ - see front matter © 2007 Elsevier Ltd. All rights reserved.
doi:10.1016/j.dyepig.2007.02.006

and boosting up the physical properties, thereby improving their performances. In this work, we reported the synthesis and characterization of a series of soluble alkyl-substituted perylene derivatives named as C4–C*n* and C4–C3–C4, which showed good solubility in common organic solvent such as $CHCl_3$, CH_2Cl_2, etc., and high thermal stability. The energy levels of the compounds were measured by cyclic voltammetry, which indicates they could be used as excellent electron-transporting materials.

2. Experimental

2.1. General

For all the reactions, magnetic stirrers were used. Commercially available reagents were used without further purification. All reactions were monitored by thin layer chromatography (TLC). Compounds were visualized with UV light at 254 and 365 nm. Melting points were measured on a WRX-1S instrument. Infrared (IR) spectra were recorded with a Perkin–Elmer spectrum one B spectrometer. ^{1}H NMR spectra were recorded on a Varian-Unity spectrometer at 500 MHz using tetramethylsilane (TMS) as an internal standard. Elemental analysis was conducted on a Flash Elemental Analyzer-Mod 1112. UV–vis absorption spectra were recorded on a Shimadzu UV-160 spectrometer. Photoluminescence was measured by Shimadzu RF-5301 PC or Perkin–Elmer LS 55 spectrometer. Cyclic voltammetry (CV) was performed on a BAS 100BW electrochemical workstation. All CV measurements were carried out in anhydrous dimethylformamide (DMF) containing 0.1 M tetrabutylammonium perchlorate (TBAP) as a supporting electrolyte, purging with nitrogen prior to conduct the experiment. Platinum wire (MF-2013) was used as a working electrode, Ag/Ag^+ as a reference electrode, and another platinum wire (MF-1032) as a counter electrode. Differential scanning calorimetry (DSC) analyses were performed on a DSC-821^e instrument. The rate of heating and cooling was 10 °C min^{-1}, the weight of the sample was about 2 mg.

2.2. Synthesis of compounds

Two types of perylene compounds named as C4–C*n* ($n = 3$, 6, 10 and 12) and C4–C3–C4 were synthesized by condensation of perylene tetracarboxylic monoanhydride monoimide with *n*-alkylbromine and/or 1,3-dibromopropane, the synthetic route is shown in Scheme 1. Their chemical structures were confirmed by FT-IR, ^{1}H NMR spectroscopies and elemental analysis.

2.2.1. Synthesis of perylene imide, C4–Cn ($n = 3$, 6, 10 and 12)

Synthesis of perylene tetracarboxylic monoimide bis-alkylester with different lengths of alkyl chains was performed through a similar procedure. A representative procedure for *n*-(1-butyl)perylene-3,4:9,10-tetracarboxylic-3,4-(bis-propylester)-9,10-imide (C4–C3) was given below [22–24].

2.2.1.1. N-(1-Butyl)perylene-3,4:9,10-tetracarboxylic-3,4-anhydride-9,10-imide (B4) [25–27]. PTCDA (1A) (3.92 g, 0.01 mol) was dispersed in 200 mL deionizing water, and

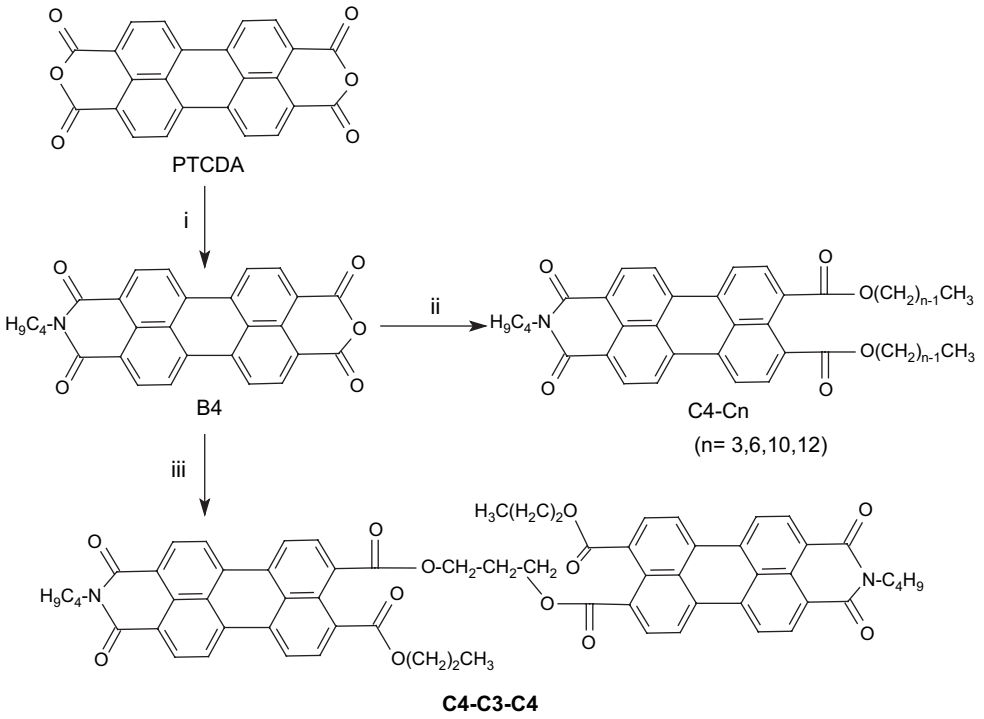

Scheme 1. (i) *n*-Butylamine, H_2O, 58–60 °C, 5 h; (ii) RBr ($R = C_nH_{2n+1}$, $n = 3$, 6, 10 and 12), *n*-propylol, K_2CO_3, reflux, 60 h; (iii) 1,3-dibromopropane, *n*-propylol, reflux, 60 h.

Table 1
The solubility properties of perylene derivatives in some solvents

Compounds	Solvents[a]								
	CH_2Cl_2	$CHCl_3$	THF	Acetone	Ether	Ethyl acetate	Ethanol	DMF	DMSO
C4–C3	+	+	+	+	+	+	+	+	+−
C4–C6	+	+	+	+	+	+	+	+	+−
C4–C10	+	+	+	+	+	+	+	+	+−
C4–C12	+	+	+	+	+	+	+	+	+−
C4–C3–C4	+	+	+−	−	−	−	+−	+	+−
PTCDA	−	−	−	−	−	−	−	−	−
B4	−	−	−	+−	−	−	−	+−	+−

[a] 0.1 mg in 1.0 mL of solvent. + soluble; +− partially soluble; − insoluble at r.t. THF: tetrahydrofuran; DMSO: dimethyl sulphoxide.

n-butylamine (9.9 mL) was added. The mixture was stirred at 58–60 °C for 5 h, and then 100 mL hydrochloric acid (HCl, 5%) was added into the reaction mixture and stirred at 80–90 °C for 1 h. The precipitate was filtered and washed with hot water several times. Then precipitate was dispersed in 300 mL potassium hydroxide hydrate (KOH, 1%) and heated to 80–90 °C for 1 h. The hot solution was filtered to remove unreacted 3,4,9,10-perylene tetracarboxylic diimides. The red precipitate was further washed with the mixture of 10% potassium chloride (KCl) and 1% potassium carbonate (K_2CO_3) until the filtrate was colorless. The product was collected through filtration and dried completely to give dark-red solid with slightly golden (B4) (yield: 42%, mp > 350 °C).

FT-IR (KBr, disc, cm^{-1}): 3099, 2957, 2932, 2875, 1767, 1723, 1694, 1656, 1594, 1507, 1435, 1406, 1380, 1351, 1270, 1241, 1152, 1088, 1073, 1017, 865, 810, 768, 755, 738, 640.

Anal. Calcd for $C_{28}H_{17}NO_5$: C, 75.16%; H, 3.83%; N, 3.13%. Found: C, 75.19%; H, 3.85%; N, 2.98%.

2.2.1.2. N-(1-Butyl)perylene-3,4:9,10-tetracarboxylic-3,4-(bis-propylester)-9,10-imide (C4–C3). *N*-(1-Butyl)perylene-3,4:9,10-tetracarboxylic-3,4-anhydride-9,10-imide (B4) (1.341 g, 3 mmol) was dissolved in 50 mL 1-propanol, then bromopropane (2.8 mL, 30 mmol) and K_2CO_3 (3.0 g) were added and refluxed at 90 °C for about 60 h. After K_2CO_3 being removed through hot filtration, 150 mL chloroform and 100 mL water were added into the filtrate and extracted for three times. The crude product was collected after removing solvent then recrystallized from alcohol and dried to give 1.05 g red solid (C4–C3) (yield: 63.7%).

^{1}H NMR ($CDCl_3$, ppm from TMS, 500 MHz): 8.64 (d, 2H), 8.50 (m, 4H), 8.13 (d, 2H), 4.32 (t, 4H), 4.22 (t, 2H), 1.86 (m, 4H), 1.83 (t, 4H), 1.48 (m, 2H), 1.05 (t, 6H), 0.99 (t, 3H).

FT-IR (KBr, disc, cm^{-1}): 3137, 1698, 1684, 1651, 1400, 1295, 1264, 1139, 1069, 952, 861, 747, 537.

Anal. Calcd for $C_{34}H_{31}NO_6$: C, 74.30%; H, 5.69%; N, 2.55%. Found: C, 74.14%; H, 5.79%; N, 2.40%.

2.2.1.3. N-(1-Butyl)perylene-3,4:9,10-tetracarboxylic-3,4-(bis-hexylester)-9,10-imide (C4–C6). Red solid (yield: 76.5%).

^{1}H NMR ($CDCl_3$, ppm from TMS, 500 MHz): 8.67 (d, 2H), 8.52 (m, 4H), 8.13 (d, 2H), 4.32 (t, 4H), 4.22 (t, 2H), 1.81 (m, 4H), 1.75 (t, 2H), 1.47 (m, 2H), 1.34 (m, 16H), 1.05 (t, 6H), 0.99 (t, 3H).

FT-IR (KBr, disc, cm^{-1}): 3138, 1698, 1684, 1652, 1400, 1298, 1263, 1141, 991, 952, 861, 807, 747, 594, 535.

Anal. Calcd for $C_{40}H_{43}NO_6$: C, 75.80%; H, 6.84%; N, 2.21%. Found: C, 75.72%; H, 6.98%; N, 2.02%.

2.2.1.4. N-(1-Butyl)perylene-3,4:9,10-tetracarboxylic-3,4-(bis-decylester)-9,10-imide (C4–C10). Red solid (yield: 45.7%).

^{1}H NMR ($CDCl_3$, ppm from TMS, 500 MHz): 8.67 (d, 2H), 8.53 (m, 4H), 8.13 (d, 2H), 4.33 (t, 4H), 4.22 (t, 2H), 1.79 (m, 4H), 1.78 (t, 2H), 1.47 (m, 2H), 1.44 (m, 4H), 1.26 (m, 28H), 1.00 (t, 6H), 0.99 (t, 3H).

FT-IR (KBr, disc, cm^{-1}): 3136, 1698, 1683, 1651, 1399, 1297, 1263, 1138, 1068, 994, 952, 863, 764, 594, 537.

Anal. Calcd for $C_{48}H_{59}NO_6$: C, 77.28%; H, 7.97%; N, 1.88%. Found: C, 77.12%; H, 8.09%; N, 1.70%.

2.2.1.5. N-(1-Butyl)perylene-3,4:9,10-tetracarboxylic-3,4-(bis-dodecylester)-9,10-imide (C4–C12). Red solid (yield: 30.2%).

^{1}H NMR ($CDCl_3$, ppm from TMS, 500 MHz): 8.67 (d, 2H), 8.53 (m, 4H), 8.14 (d, 2H), 4.33 (t, 4H), 4.22 (t, 2H), 1.79 (m, 4H), 1.77 (t, 2H), 1.47 (m, 2H), 1.44 (m, 4H), 1.25 (m, 28H), 1.00 (t, 6H), 0.99 (t, 3H).

FT-IR (KBr, disc, cm^{-1}): 3137, 1698, 1683, 1650, 1400, 1293, 1264, 1141, 991, 951, 861, 807, 747, 536.

Anal. Calcd for $C_{52}H_{67}NO_6$: C, 77.87%; H, 8.42%; N, 1.75%. Found: C, 77.79%; H, 8.38%; N, 1.63%.

2.2.2. Synthesis of perylene imide dimer, 1,3-bis[(n-(1-butyl)perylene-3,4:9,10-tetracarboxylic-3-alkylester-9,10-imide)-4-ester] dioxypropane (C4–C3–C4)

B4 (1.34 g, 3 mmol) was dissolved in 50 mL 1-propanol, then 1,3-dibromopropane (3.02 g, 15 mmol) and K_2CO_3 (3 g) were added and refluxed at 80–90 °C for about 60 h. After K_2CO_3 being removed through hot filtration, 150 mL chloroform and 100 mL water were added into the filtrate and extracted for three times. The resulting mixture was subjected to chromatography separation (using 20:1 chloroform/alcohol as the eluent) to recover dark-red solid (C4–C3–C4) (yield: 25.2%).

^{1}H NMR ($CDCl_3$, ppm from TMS, 500 MHz): 8.32 (m, 2H), 8.15 (m, 3H), 7.77 (d, 1H), 7.68 (d, 1H), 7.47 (d, 1H), 4.65 (t, 4H), 4.33 (t, 4H), 4.17 (t, 4H), 2.40 (t, 2H), 1.86 (m, 4H), 1.72 (m, 4H), 1.48 (m, 4H), 1.07 (t, 6H), 1.00 (t, 6H).

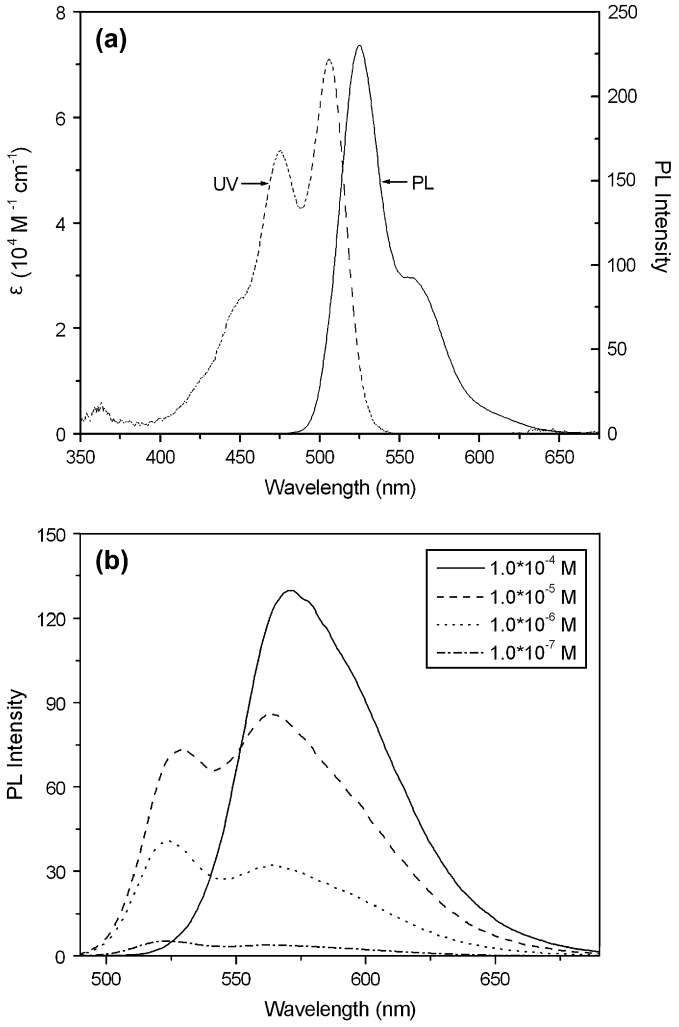

Fig. 1. UV–vis absorption and fluorescence spectra of C4–C3 in chloroform at 10^{-6} M (excitation wavelength was 510 nm) (a) and concentration-dependent fluorescence spectra of C4–C3–C4 in chloroform (excitation wavelength was 480 nm) (b).

FT-IR (KBr, disc, cm^{-1}): 2962, 2869, 1718, 1698, 1654, 1594, 1511, 1457, 1430, 1416, 1383, 1357, 1296, 1264, 1214, 1199, 1173, 1079, 1038, 964, 849, 808, 748, 580.

Anal. Calcd for $C_{65}H_{54}N_2O_{12}$: C, 73.99%; H, 5.16%; N, 2.65%. Found: C, 73.75%; H, 5.27%; N, 2.49%.

3. Results and discussion

3.1. Synthesis

The synthetic route shown in Scheme 1 describes the preparation of two different perylene derivatives through the condensation of perylene tetracarboxylic monoanhydride monoimide with alkylbromine. As can be seen from the synthetic scheme, the condensation of the dianhydride PTCDA with *n*-butylamine will result two products, e.g., the perylene tetracarboxylic monoanhydride monoimide named B4 and the bis-(dicarboximide) B4′. Both B4 and B4′ were separated from PTCDA by dissolving the mixture in a mixed aqueous solution of potassium hydroxide and potassium chloride, in which PTCDA is soluble. The monoimide B4 can be obtained by treatment of the residue containing B4 and B4′ with hot dilute aqueous solution of potassium hydroxide and acidification after removing B4′. The monoanhydride monoimide B4 exhibited $\nu_{c=o}$ of anhydride at 1767 and 1723 cm^{-1} and $\nu_{c=o}$ of imide at 1694 and 1656 cm^{-1}, while bis-(dicarboximide) B4′ showed $\nu_{c=o}$ of imide at 1694 and 1657 cm^{-1}. Further condensation of perylene tetracarboxylic monoanhydride monoimides with *n*-alkylbromine (alkyl = propyl, hexyl, decyl and dodecyl) and/or 1,3-dibromopropane in 1-propanol resulted in monoimide bis-alkylesters C4–C*n* and C4–C3–C4. The $\nu_{c=o}$ of bis-alkylester monoimide C4–C*n* centered at 1680–1700 cm^{-1} (C=O of ester) and at 1650–1655 cm^{-1} (C=O of imide). While, the $\nu_{c=o}$ of the dimer C4–C3–C4 located at 1718, 1698 and 1654 cm^{-1}. Introduction of long alkyl chains to perylene core, via unusual ester bonding instead of the traditional imide bonding, substantially improves the solubility and lowers the melting points of the compounds with respect to the dodecyl-substituted diimide that melts above 325 °C and is appreciably soluble only in refluxing solvents such as chlorobenzene.

The solubility of the perylene derivatives in different solvents was measured at concentration 0.1 mg mL^{-1} at room temperature (see Table 1). Differing from PTCDA and B4, which are insoluble or poorly soluble in organic solvents [28], C4–C*n* and C4–C3–C4 are soluble in common organic solvents such as chloroform and dichloromethane, etc., at room temperature. The improvement in solubility of the present perylene derivatives may be attributed to the introduction

Table 2
The absorption and fluorescence data of C4–C*n* and C4–C3–C4

Compounds	λ_{max} of absorbance in chloroform (nm)	Absorption coefficient in chloroform, λ_{max} (nm) and ε (10^4 M^{-1} cm^{-1}) (in parenthesis)	λ_{max} of emission in chloroform[a] (nm)
C4–C3	474, 505	474 (5.36), 505 (7.09)	523, 560
C4–C6	474, 506	474 (6.18), 506 (8.03)	524, 560
C4–C10	474, 505	474 (6.52), 505 (8.37)	524, 562
C4–C12	473, 506	473 (6.32), 506 (8.18)	526, 560
C4–C3–C4	476, 507	476 (9.72), 506 (7.94)	525, 568
PTCDA[b]	500, 530		

[a] The concentration of compounds in solution was 10^{-6} M for C4–C*n* and C4–C3–C4, excitation wavelength was 480 nm.
[b] Value is in acidic solution.

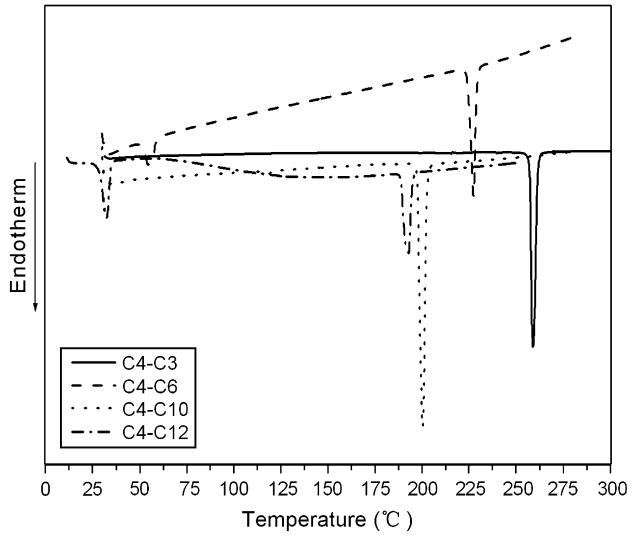

Fig. 2. Differential scanning calorimeter traces for C4–C*n* ($n = 3$, 6, 10 and 12) during the second heating (heating rate: 10 °C min^{-1}).

of long alkyl chain and ester groups that reduced the interaction between perylene rings.

3.2. Optical properties

Fig. 1a shows the absorption and fluorescence spectra of C4–C3 in chloroform at dilute concentration (10^{-6} M). A shoulder and two absorbance peaks centered at 450, 474 and 505 nm were attributed to the transitions of $0 \rightarrow 2$, $1 \rightarrow 2$ and $0 \rightarrow 1$, respectively, while two maximum emissions were observed at 523 ($0 \rightarrow 0$) and 560 nm ($0 \rightarrow 1$), with the Stokes-shift of 18 nm. The fluorescence spectra of C4–C3–C4 in chloroform at concentrations in the range of 1.0×10^{-4} and 1.0×10^{-7} M are shown in Fig. 1b. One emission at 570 nm was observed for C4–C3–C4 at relatively higher concentration (10^{-4} M), on the contrary, the PL spectra exhibited two emissions at 563 and 503 nm at much lower concentrations (10^{-6} M) and the relative intensities of the $0 \rightarrow 1$ (563 nm) and $0 \rightarrow 0$ (523 nm) transitions are reversed with decreasing concentration to 10^{-7} M, which is similar to that of C4–C*n*, indicating that C4–C3–C4 molecules are aggregated in cofacial π–π stack geometry [29]. The photophysical properties of C4–C*n* ($n = 3$, 6, 10 and 12) and C4–C3–C4 are summarized in Table 2. The lowest energy absorption bands are from the π–π* transitions by virtue of their large molar extinction coefficients. The UV–vis absorption spectra of C4–C*n* and C4–C3–C4 are nearly identical, whose maximum absorption wavelength (λ_{max}) are at around 475 and 506 nm, independent of the length of alkyl chains.

Thermal properties of C4–C*n* and C3–C4–C3 were investigated by DSC analysis. The DSC curves of C4–C6 and C4–C12 showed two endothermic transitions corresponding to crystalline–crystalline and crystalline–isotropic transition, while for C4–C3 and C4–C10, only one transition attributing to crystalline–isotropic transition was observed (see Fig. 2). The assignment of the transition was further confirmed by polarized optical microscopy and wide-angle X-ray diffraction (WAXD) measurement. The crystalline transition temperatures and associated enthalpic changes for C4–C*n* ($n = 3$, 6, 10 and 12) and C4–C3–C4 are summarized in Table 3. C4–C3, C4–C6, C4–C10 and C4–C12 melt at 258.4,

Table 3
The calorimetric data for C4–C*n* and C4–C3–C4

Compounds	T/°C (ΔH/kJ mol^{-1})	
	Heating[a]	Cooling
C4–C3	258.4 (29.84)	244.6 (30.16)
C4–C6	54.3 (8.62), 227.4 (28.57)	220.6 (29.1), 47.7 (7.27)
C4–C10	199.5 (30.26)	192.2 (31.72)
C4–C12	32.2 (22.73), 192.8 (32.94)	185.0 (32.64), 15.6 (20.15)
C4–C3–C3–C4	$T_m = 313$, decomposed at 350 °C	

[a] Heating rate: 10 °C min^{-1}.

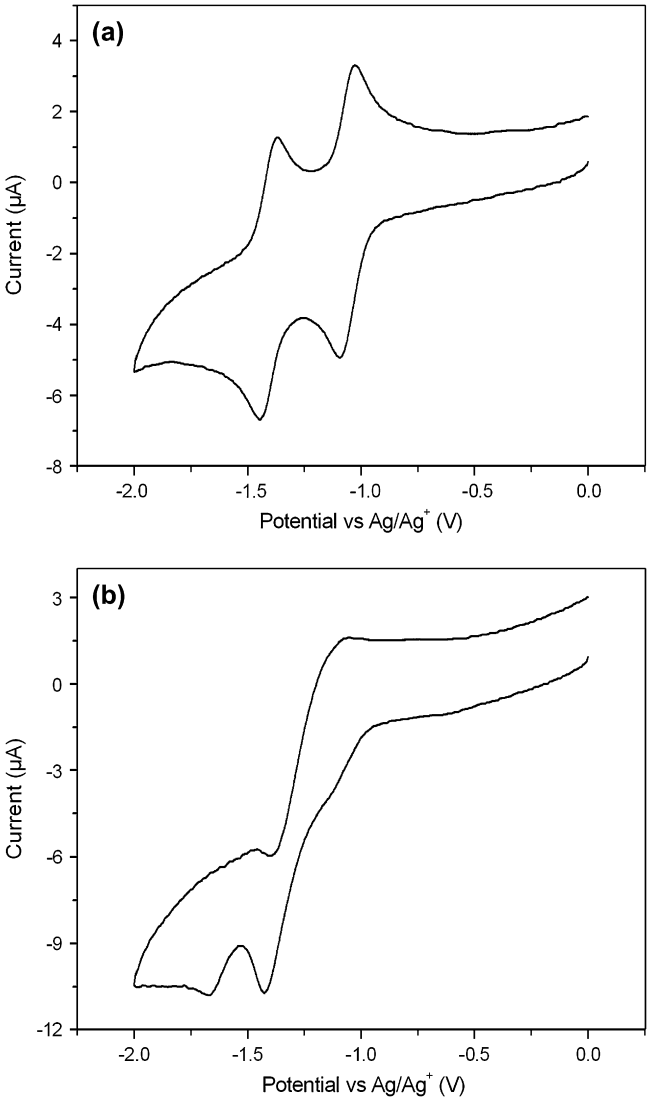

Fig. 3. Cyclic voltammetry curves of C4–C6 (a) and C4–C3–C4 (b) (in DMF/supporting electrolyte: TBAP, scan rate: 50 mV s^{-1}).

Table 4
The redox potential, HOMO and LUMO energy levels and band gaps of C4–C*n* and C4–C3–C4 measured in DMF

Compounds	E_{1r} (V)		E_{2r} (V)		Energy (eV, experimental[a])			Energy (eV, calculated[c])		
					E_{HOMO} (IP)[b]	E_{LUMO} (EA)	E_g^{opt}	E_{HOMO}	E_{LUMO}	E_g
C4–C3	−1.10	−1.03	−1.45	−1.38	−6.08	−3.78	2.30			
C4–C6	−1.09	−1.02	−1.45	−1.37	−6.10	−3.79	2.31	−5.43	−3.85	1.58
C4–C10	−1.10	−1.05	−1.49	−1.38	−6.09	−3.78	2.31			
C4–C12	−1.10	−1.04	−1.30	−1.18	−6.07	−3.76	2.31			
C4–C3–C4	−1.12	−1.06	−1.42	−1.39	−5.96	−3.76	2.20	−5.21	−3.68	1.53
PTCDA [30]					−9.33	−2.95	6.38			

[a] Energy level was determined from the formula: $E_{HOMO} = eE_{ox} + 4.5$ eV and $E_{LUMO} = -eE_{red} - 4.5$ eV, where E_{ox} and E_{red} are the oxidation and reduction potentials in volts vs. the normal hydrogen electrode potential. Electrochemical band gap $E_g = E_{LUMO} - E_{HOMO}$. Optical band gap E_g^{opt} was calculated from the optical absorption spectra.
[b] For C4–C*n* and C4–C3–C4, the HOMO energies are estimated according to the E_g^{opt} and the LUMO energies from electrochemical experimental results.
[c] Calculated from Dmol^3 package of MS Modeling 3.0 through the geometry optimization using GGA method with PW91 function.

227.4, 199.5 and 192.8 °C, respectively. Obviously, introduction of alkyl chain to the perylene core lowered the melting temperature; the longer the alkyl groups, the lower the melting points. C4–C3–C4 melts at 313 °C and decomposes at 350 °C.

3.3. Electrochemical properties

The electrochemical properties of the perylene derivatives were investigated by cyclic voltammetry (CV) in DMF. The CV curves of C4–C6 and C4–C3–C4 are shown in Fig. 3, and Table 4 summarizes LUMOs calculated from CV and band gaps (E_g^{opt}) estimated from the maximum absorption wavelength (λ_{max}). The measured LUMOs and calculated HOMOs of C4–C3, C4–C6, C4–C10, C4–C12 and C4–C3–C4 are −3.78, −3.79, −3.78, −3.76, −3.76 eV and −6.08, −6.10, −6.09, −6.07, −5.96 eV, respectively, which suggested that the two types of perylene derivatives exhibited analogous energy levels in spite of their different chemical structures, e.g., it is the conjugated structure not the alkyl chains that determined the energy levels as well as the band gaps. The LUMO and HOMO energy levels of the compounds studied were in the range of −3.79 to −3.76 eV and −6.10 to −5.96 eV, which indicates that they should show good performance as electron-transporting/hole-blocking materials.

3.4. Electronic structure

Calculations of the electronic structure of C4–C6 and C4–C3–C4 were performed by the Dmol^3 package of MS Modeling 3.0 through the geometry optimization using GGA method with PW91 function. The corresponding electron density diagrams of the HOMO and LUMO are depicted in Fig. 4, and the frontier molecular orbital energies are summarized in Table 4. The calculations showed that electrons distributed among the whole perylene ring for LUMOs and HOMOs of C4–C6 while those of C4–C3–C4 mainly located on one of the two perylene rings, similar to that of C4–C*n*. It is because the conjugation of the two perylene rings in C4–C3–C4 is disrupted by the alkyl chain. The HOMOs of C4–C*n* (ca. −6.10 eV) are almost similar to that of C4–C3–C4 (−5.96 eV), much higher than that of PTCDA (−9.33 eV). In the meanwhile, it can be seen that the LUMO electron density diagrams of C4–C*n* and C4–C3–C4 are almost identical and their LUMOs (ca. −3.80 eV) are lower than that of PTCDA (−2.95 eV). As a result, the HOMO–LUMO energy

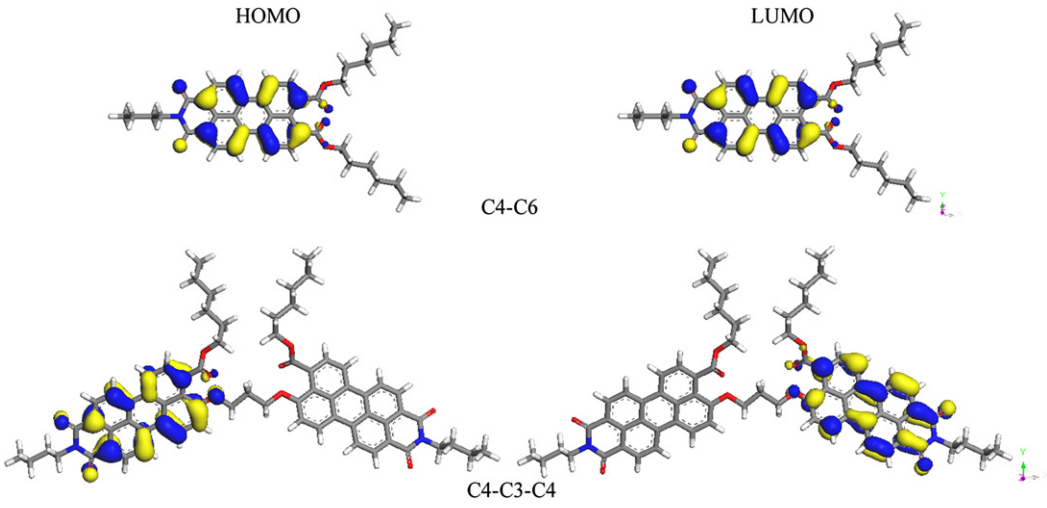

Fig. 4. The electron density diagram of the frontier molecular orbital of C4–C6 and C4–C3–C4.

gaps decrease on going from PTCDA to C4–C3–C4. This result is consistent with the fact that the lower energy absorption of C4–C3–C4 (at 510 nm) red-shifted compared with that of PTCDA (at 530 nm).

The higher HOMO energy levels of C4–C6 (−6.10 eV) and C4–C3–C4 (−5.96 eV) than that of PTCDA (−9.33 eV) should lead C4–C6 and C4–C3–C4 much easier to be oxidized than PTCDA. Alkyl substituents and ester group affect the electron donating and accepting abilities of the species through the perturbation to the frontier molecular orbital. Conclusively, the electron-transporting characteristics as an OLED material are effectively improved.

4. Conclusions

We have successfully prepared and characterized new perylene derivatives. Introduction of alkyl chain and ester groups to perylene core enhanced their solubility in common organic solvents. The photoluminescent maxima of the perylene compounds in solution located at 520–570 nm. All the compounds studied show quasi-reversible redox behavior, the LUMO and HOMO energy levels are in the range of −3.76 to −3.79 eV and −5.96 to −6.10 eV. Both HOMO and LUMO energy levels of C4–C*n* and C4–C3–C4 were almost identical, different from that of PTCDA. It was indicated that these compounds are suitable candidates for electron-transporting materials in electronic devices.

Acknowledgments

This work was supported by the National Science Foundation committee of China (Project No. 50373016), Program for New Century Excellent Talents in Universities of China Ministry of Education, and Special Foundation for Ph.D. Program in Universities of China Ministry of Education (Project No. 20050183057).

References

[1] Liu D, De Feyter S, Cotlet M, Stefan A, Wiesler UM, Herrmann A, et al. Macromolecules 2003;36:5918–25.
[2] Würthner F. Chem Commun 2004;1564–79.
[3] Seguy I, Jolinat P, Destruel P, Farenc J, Mamy R, Bock H, et al. J Appl Phys 2001;89(10):5442–8.
[4] Rainer D, Marina L, Pablo B, Matthias G, Frank W. Macromolecules 2005;38:1315–25.
[5] O'Neil MP, Niemczyk MP, Svec WA, Gosztola D, Gaines III GL, Wasielewski MR. Science 1992;257(III):63.
[6] Schneider M, Hagen J, Haarer D, Műllen K. Adv Mater 2000;12(5): 351–4.
[7] Ranke P, Rleyl I, Simmerer J, Haarer D, Bacher A, Schmidt HW. Appl Phys Lett 1997;71:1332–4.
[8] Osman MA, Zeller HR, Markert J. EP 47027; 1982.
[9] Benning SA, Hassneider T, Keuker-Baumann S, Bock H, Della Sala F, Frauenheim T, et al. Liq Cryst 2001;28(7):1105–13.
[10] Moryson H, Kozlowski K, Bauman D. Mol Cryst Liq Cryst 1999;331:2299–307.
[11] Bauman D, Mykowska E, Wolarz E. Mol Cryst Liq Cryst 1998;321: 777–91.
[12] Haßheider T, Benning SA, Lauhof MW, Kitzerow HS, Bock H, Watson MD, et al. Mol Cryst Liq Cryst 2004;413:2597–608.
[13] Tang CW. Appl Phys Lett 1986;48:183–5.
[14] Oukachmih M, Destruel P, Seguy I, Ablart G, Jolinat P, Archambeau S, et al. Sol Energy Mater Sol Cells 2005;85(4):535–43.
[15] Yakimov A, Forrest SR. Appl Phys Lett 2002;80:1667–9.
[16] Breeze AJ, Salomn A, Ginley DS, Gregg BA, Tillmann H, Hörhold HH. Appl Phys Lett 2002;81:3085–7.
[17] Schmidt-Mende L, Fechtenkötter A, Műllen K, Moons E, Friend RH, MacKenzie JD. Science 2001;293:1119.
[18] Qu JQ, Zhang JY, Grimsdale AC, Müllen K. Macromolecules 2004;37:8297–306.
[19] Schlichting P, Rohr U, Műllen K. Eur J Org Chem 1997;2:395–407.
[20] Pan JF, Zhu WH, Li SF, Xu J, Tian H. Eur J Org Chem 2006;986–1001.
[21] Pan JF, Zhu WH, Li SF, Zeng WJ, Cao Y, Tian H. Polymer 2005;46:7658–69.
[22] Benning S, Kitzerow HS, Bock H, Achard MF. Liq Cryst 2000;27(7):901–6.
[23] Seguy I, Jolinat P, Destrael P, Mamy R, Allouchi H, Courelle C. ChemPhysChem 2001;2(7):448–52.
[24] Pasaogullari N, Icil H, Demuth M. Dyes Pigments 2006;69:118–27.
[25] Tröster H. Dyes Pigments 1983;4:171–7.
[26] Nagao Y. Prog Org Coat 1997;31:43–9.
[27] Langhals H, Jona W. Eur J Org Chem 1998;847–51.
[28] Huang W, Yan DY, Lu QH, Huang Y. Eur Polym J 2003;39(6): 1099–104.
[29] Yan P, Chowdhury A, Holman MW, Adams DM. J Phys Chem B 2005;109:724–30.
[30] Mercadante R, Trsic M, Duff J, Aroca R. J Mol Struct 1997;394: 215–26.